

WMO AIRBORNE DUST BULLETIN

No. 4 | May 2020

WMO Sand and Dust Storm – Warning Advisory and Assessment System (SDS-WAS)

Sand and dust storms (SDSs) have been recognized by recent United Nations General Assemblies and World Meteorological Congresses as severe hazards that can affect weather, climate, the environment, health and economies in many parts of the world. To combat these hazards, operational SDS forecasting, warning advisory and information assessment services need to be provided for various regions of the world in a globally coordinated and harmonized manner. Since 2004, and at the request of more than 40 countries, WMO has taken the lead in this area and established the Sand and Dust Storm Warning Advisory and Assessment System (SDS-WAS) to develop, refine and provide a basis for distributing to the global community products that can be used to reduce the adverse impacts of SDSs and to assess the effects of SDSs on societies and on the environment.

In June 2019, the Eighteenth World Meteorological Congress approved Resolution 19 (Cg-18) – Enhancing cooperation for monitoring and forecasting sand and dust storms. Congress noted the progress made regarding the implementation of SDS-WAS and suggested that Member Countries promote international cooperation to combat SDSs through the exchange of knowledge, experiences and best practices and by offering training courses. Congress also suggested that Member Countries enhance their capacity-building efforts and their provision of technical assistance in order to monitor and forecast SDSs and to support the implementation of the national, regional and global action plans of affected countries.

Overview of atmospheric dust content in 2019

The spatial distribution of the global surface concentration of mineral dust in 2019 (Figure 1) and its anomaly relative to climatologically mean values (1981–2010) (Figure 2) were derived based on the dust products from the Modern-Era Retrospective Analysis for Research and Applications, Version 2 (MERRA-2) (Gelaro et al., 2017), the latest atmospheric reanalysis version for the modern satellite era produced by NASA's Global Modeling and Assimilation Office (GMAO). MERRA-2 includes an online implementation of the Goddard Chemistry, Aerosol, Radiation, and Transport model (GOCART) integrated into the Goddard Earth Observing System Model, Version 5 (GEOS-5) and is capable of simulating five types of aerosols. The results shown here are based on the dust surface concentration parameter, which is different from the dust aerosol optical depth (DAOD) parameter and more relevant to ground air quality.

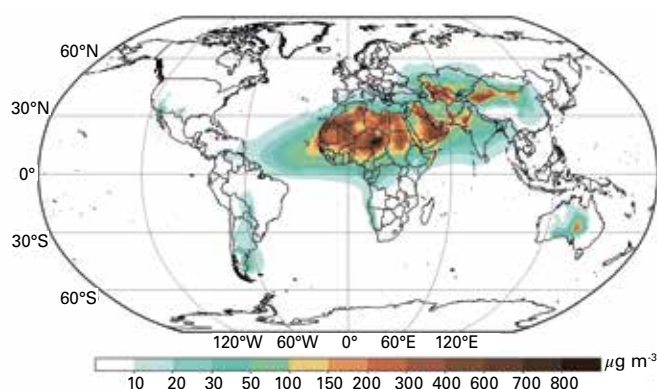


Figure 1. Annual mean surface concentration of mineral dust in 2019

Generally, the spatial distribution of the global surface concentration of mineral dust in 2019 was similar to that present in 2018 (see Airborne Dust Bulletin No. 3, Zhang et al., 2019). In 2019, a well-known dust belt, composed of primary dust sources, including northern and Central Africa, the Arabian Peninsula, northern India, Central Asia, and the deserts in north-western and northern China could clearly be seen in the northern hemisphere (Figure 1). The estimated peak dust concentration ($\sim 900\text{--}1100\ \mu\text{g}/\text{m}^3$) was found in some areas of Chad in Central Africa. High dust concentrations were also seen in some regions in the Arabian Peninsula, Central Asia, the Iranian Plateau, and north-western China (mass concentrations of $\sim 300\text{--}600\ \mu\text{g}/\text{m}^3$). Dust concentrations reached their highest level in the southern hemisphere ($\sim 200\ \mu\text{g}/\text{m}^3$) in parts of Central Australia and the west coast of South Africa. From these locations, dust was transported to the surrounding regions, including the northern tropical Atlantic Ocean between West Africa and the Caribbean, South America, the Mediterranean Sea, the

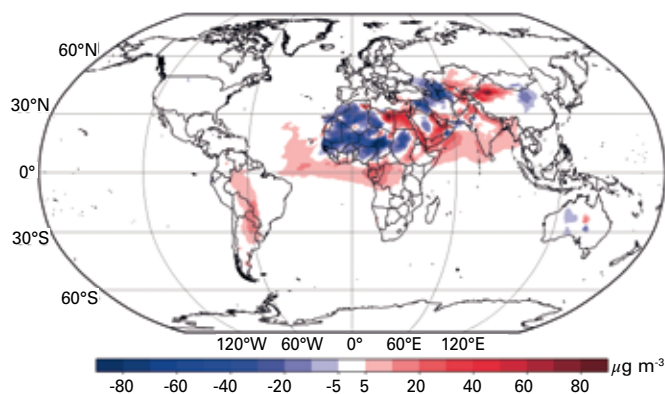


Figure 2. Anomaly of the annual mean surface dust concentration in 2019 relative to the 1981–2010 mean

Arabian Sea, the Bay of Bengal, central-eastern China, the Korean Peninsula and Japan, demonstrating the significant impact of SDSs on many regions of the world.

In most dust plume-affected areas, the surface dust concentration in 2019 was higher than the climatological mean; exceptions to this were the regions of North Africa, including Mauritania, Mali, Algeria, western Libya, Sudan, Niger, Nigeria and Chad; Central Asia; Central Arabia; Iraq; central-northern China; and central-western Australia (Figure 2). Hot spots with significantly higher dust concentrations included Egypt, north-eastern Libya, the Red Sea, southern Arabia, and north-western China.

The three-dimensional vertical distribution of the dust extinction coefficient (DEC) in the spring of 2019 (Figure 3) was derived based on the level 3 tropospheric aerosol profile product (CAL_LID_L3_Tropospheric_APro-Standard-V4-20) from CALIPSO lidar (Tackett et al., 2018). The results presented here are the average values for daytime and night-time under the all-sky condition. Satellite observations in the spring of 2019 provide direct evidence of intense mineral dust activity (such as the trans-Pacific and trans-Atlantic transport of mineral dust aerosols) throughout much of the northern hemisphere. Active DEC (extinction $> 0.1 \text{ km}^{-1}$) can be observed over North Africa, the Arabian Peninsula, north-western China, and the Indian subcontinent, which is mainly located at an altitude range of 1–3 km above mean sea level (a.s.l). The maximum height of the dust plume layer (DEC $> 0.001 \text{ km}^{-1}$) was around 5–6 km a.s.l, spanning the area between 10°N and 50°N; this demonstrates the long-range transport features of SDSs in the world's major source areas.

Several severe SDS events that occurred in these hot spots in 2019 and which are presented below resulted in deaths and serious social and economic losses.

Major SDS events over various regions of the world in 2019

SDSs over the Persian Gulf and Arabian Peninsula

This situation on 17 January 2019 was representative of the many SDSs affecting Persian Gulf and Arabian Peninsula countries during the year (Figure 4). The satellite images show a dust cloud advancing at high speed over Iraq, Iran, Kuwait, the Kingdom of Saudi Arabia and Bahrain. Widespread dust affected the region, with strong north-westerly winds causing

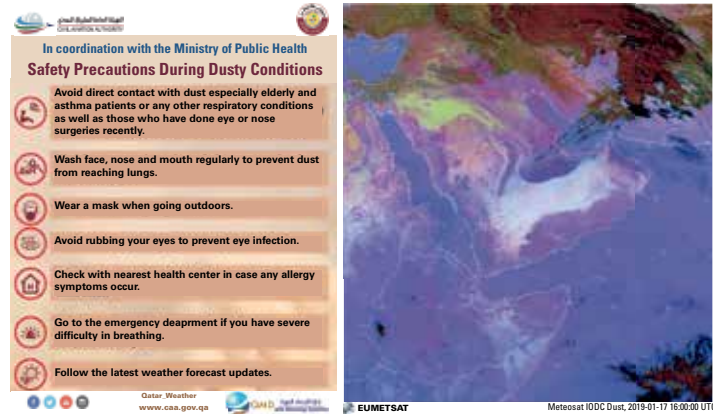


Figure 4. SDS warning issued on 17 January 2019 by Qatar authorities: Please take extra care and follow the attached safety tips as dusty conditions are expected to continue until night-time. (Source: Qatar Civil Aviation Authority; EUMETSAT)

visibility to drop below 1 km in most areas (for example, Bahrain: 800 m, Al-Ahsa: 200 m, Dammam: 50 m, Kuwait: 500 m, Abadan: 500 m, Al Udeid Air Base, Doha International Airport: 700 m). The NMMB-MONARCH operational model (formerly the NMMB-BSC model) forecast the SDS and proved to be a useful tool to prevent SDS impacts (Figure 5).

Dust intrusion over the Mediterranean Sea on 25 January 2019

A low-pressure area over the Mediterranean Sea carried airborne dust raised in northern Africa towards Greece and Turkey. The forecast (<https://dust.aemet.es/forecast>) indicated that the dust cloud would sweep across Turkey and Eastern Europe. Satellite images (Figure 6) showed good agreement with the output of the Barcelona Dust Forecast Center NMMB-MONARCH operational model (Figure 7).

Asian SDS episode in October

The SDS episode with the most significant impact in 2019 occurred from 27 to 30 October and led to abundant dust aerosols affecting vast areas of northern China, including central and western Inner Mongolia, Gansu, Ningxia, central and north Shaanxi, Shanxi, Hebei, Beijing, Henan, Anhui, Jiangsu and Shandong. Moreover, the residential time of the

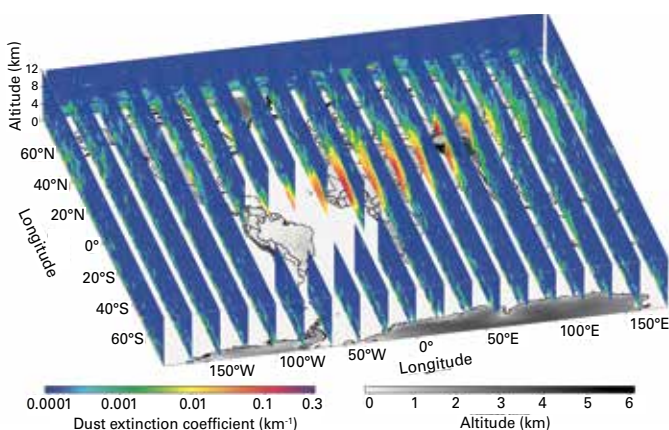


Figure 3. CALIPSO-derived global three-dimensional vertical distribution of the dust extinction coefficient (DEC) in the spring of 2019. Selected latitude-vertical cross-sections (along longitudes at 20° intervals) are shown for a better view.

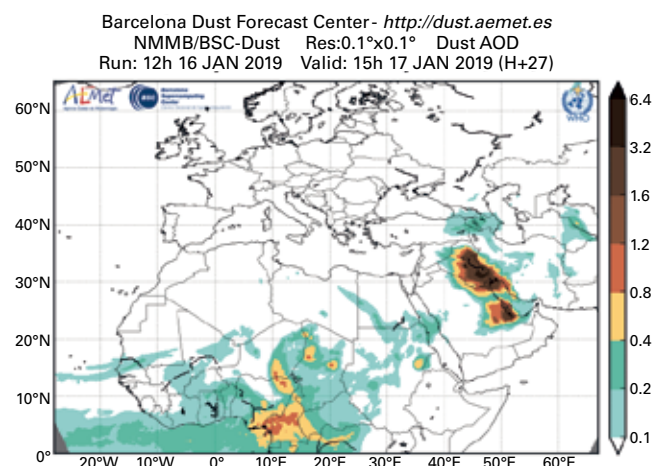


Figure 5. Dust AOD forecast for 17 January 2019, 1500 UTC. (Source: Barcelona Dust Forecast Center)

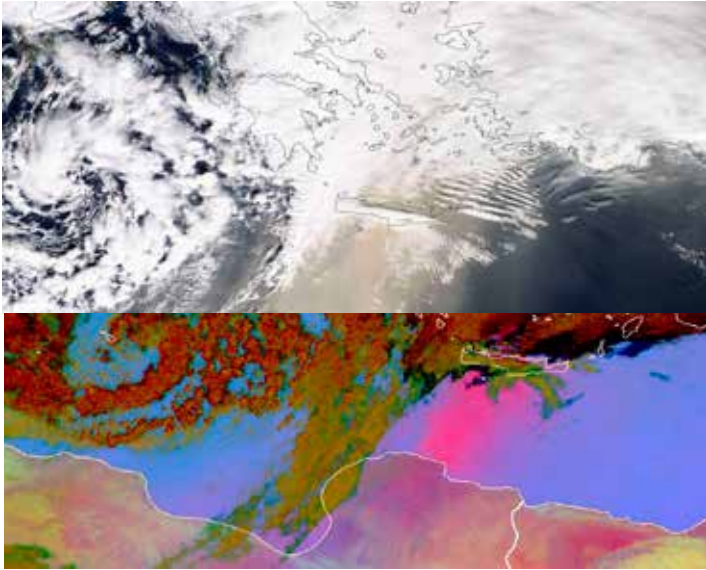


Figure 6. Dust outbreak to Europe as seen by Terra/MODIS (25 January 2019) (Source: NASA) and METEOSAT RGB (25 January 2019, 0515 UTC) (Source: EUMETSAT)

sand and dust particles during this severe episode, which occurred in the autumn when SDSs are rare in China, was relatively long in downwind areas (two to three days in the Huang River and Huai River areas, as well as in the Yangtze River and Huai River areas).

The operational numerical forecasting systems of the Beijing Dust Forecast Centre in the SDS-WAS Asian Node forecast this SDS episode well one to two days in advance (<http://www.asdf-bj.net/>). The ensemble of Node models best forecast the high dust concentrations in Shaanxi, Shanxi, Hebei, Beijing and Henan two days in advance; this corresponded well with the later observed SDS concentrations in those regions (Figure 8).

Australian SDS event

2019 was the hottest and driest year on record in Australia, and in the first weeks of 2020, a series of major dust storms formed over dust sources in the central part of the subcontinent. The Australian Bureau of Meteorology issued a dust storm warning on 22 January, predicting “damaging winds of 60–70 km/h with gusts of 90 km/h” associated with thick raised dust. Later that day, a dust storm moved

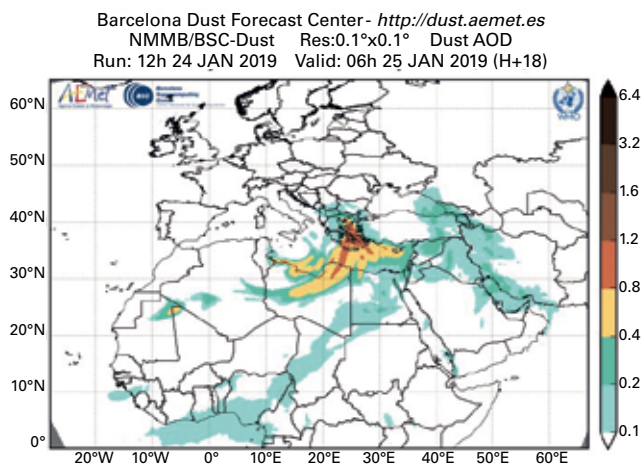


Figure 7. Dust AOD forecast for 25 January 2019, 0625 UTC. (Source: Barcelona Dust Forecast Center)

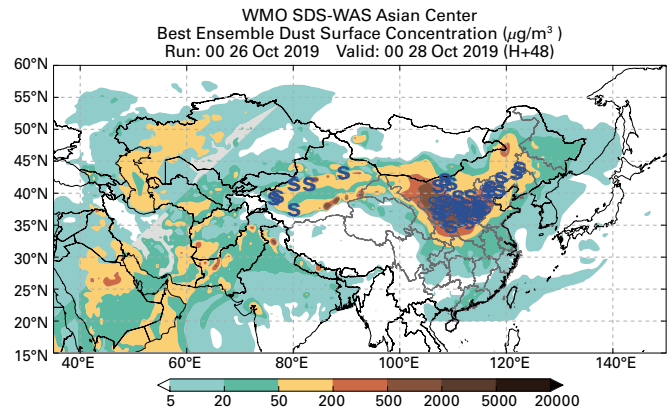


Figure 8: Comparison between observed SDS concentrations and forecast dust surface concentrations ($\mu\text{g}/\text{m}^3$) by best ensemble forecast at 0000 UTC on 28 October 2019 from the Asian Node. Blue symbols (S) indicate the weather stations where dust was recorded. (Source: Beijing Dust Forecast Centre)

through New South Wales and over parts of Victoria to arrive in Melbourne. The air became orange, and visibility dropped significantly. It became almost impossible to drive (Figure 9). After two days, the dust pattern moved southward to cover a large part of Antarctica’s eastern coast. A dust prediction indicated that the dust arrived on 24 January in Antarctica and covered a large portion of the continent’s eastern coastline.

The accelerated warming in the Arctic and Antarctica (<https://www.ipcc.ch/2019/09/25/srocc-press-release/>) is caused by numerous processes in which aerosols play a significant role at high latitudes. Dust, in particular, changes snow/ice albedo and melting rates, affects marine productivity, alters microbial dynamics in glaciers and causes indirect (cloud formation) and direct (solar radiation) effects. Studying dust storms, such as the January episode, should help us to better understand the rapid climate change occurring at high latitudes.

Pan-American SDS event

Several dust plumes travelled across the Atlantic Ocean in late June 2019. One plume was forecast to make its way through the Caribbean Sea and reach the Gulf Coast of the United States of America starting 22–25 June. This made



Figure 9. Australian landscape in the middle of the dust storm of 22 January 2020 (<https://www.abc.net.au/news/2020-01-22/dust-storm-engulfs-parts-of-outback-sa-victoria-and-nsw/11890320>)

for interesting sunsets on the gulf coast of Florida and hazy conditions over cities such as Austin and Houston, Texas (Figure 10).

Research highlights of 2019

PRIORITY AREA: Address limitation

REDETECTION OF DUST SOURCES IN THE ASIAN AREA

The accuracy of dust emission is determined in particular by the erosion database, which includes detailed soil (size distribution, texture and composition) and land surface information. Major efforts have been made to improve the quality of global dust source distribution information through satellite aerosol optical depth (AOD) data (Ginoux et al., 2012). SDS observations from meteorological stations for 2000–2017 were used to update the source database. The readjusted dust source data improve the forecast of the CUACE/Dust model in the Beijing Dust Forecast Centre in terms of both large-scale SDS episodes and microphysics in emission, station mass concentrations and size distributions (Figure 11).

EXPERIMENTAL ICE NUCLEATION PREDICTIONS

The formation of cold clouds is enhanced if ice nuclei (IN) are available. Observations show that mineral dust



Figure 10. A photo of the sunset seen from Lee County, Florida. On 25 June 2019, Saharan dust transported across the Atlantic Ocean and the Gulf of Mexico caused hazy conditions. (Credit: Andrew West/The News-Press)

particles are the dominant residuals found in cloud ice (see, for example, Cziczo et al., 2013). The regional dust DREAM model in the Republic Hydrometeorological Service of Serbia has been extended by adding a parameterization of IN (Nickovic et al., 2016; Nickovic et al., 2015) using simulated dust concentration, moisture and temperature (Demott et al., 2015; Steinke et al., 2016). This is a first step

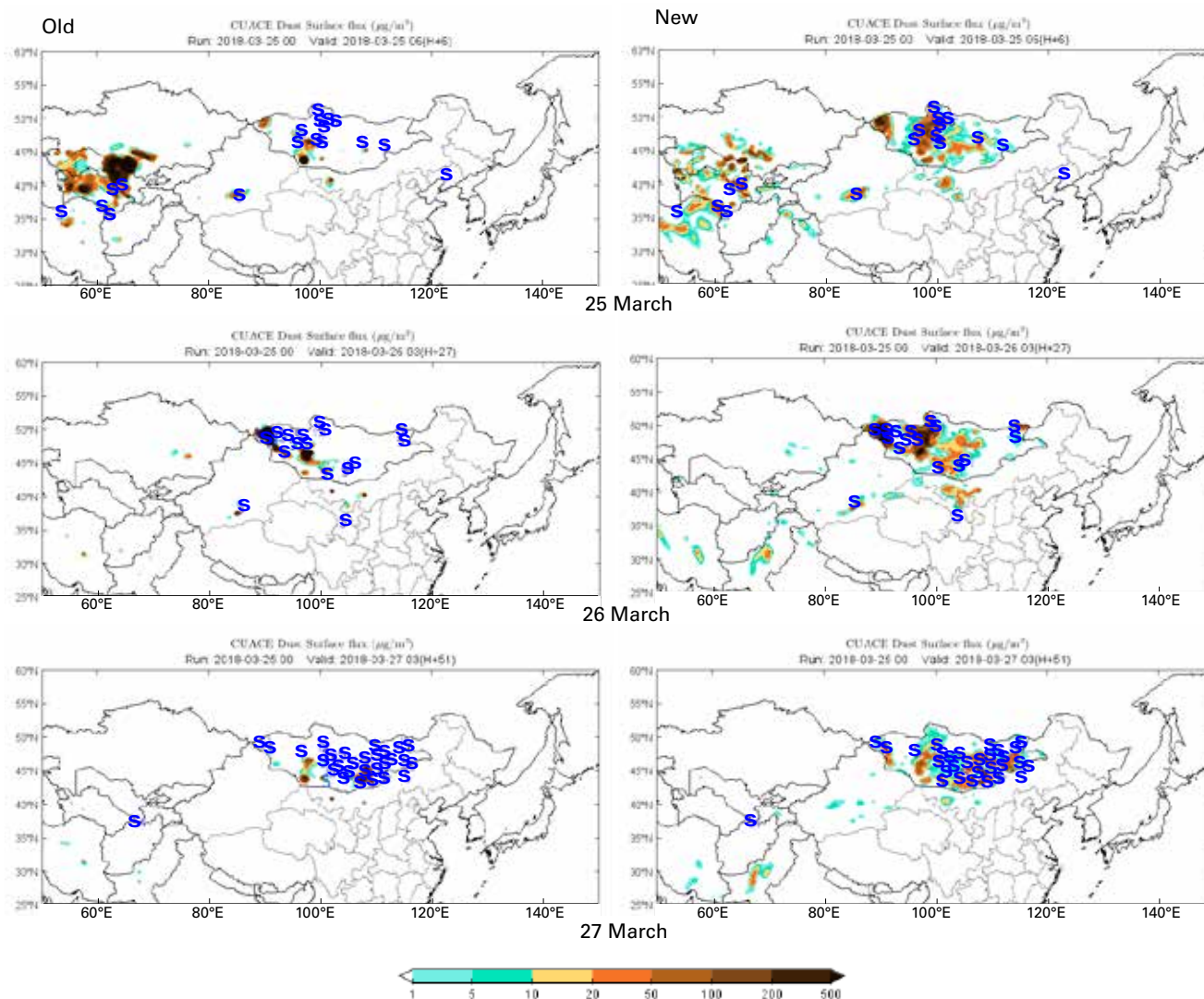


Figure 11. New dust sources detected and their impact on simulations of severe SDSs in Asia. Blue symbols (S) indicate the weather stations where dust was recorded. (Source: Zhou, C. et al., 2019)

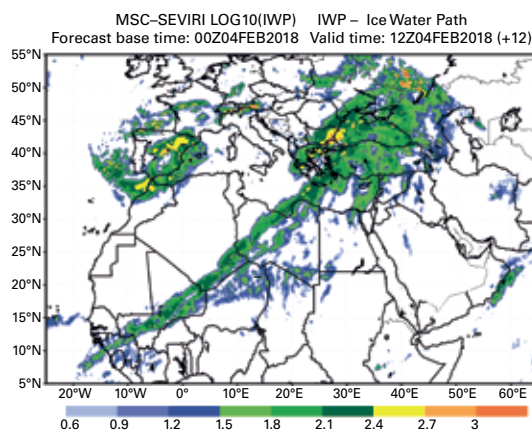
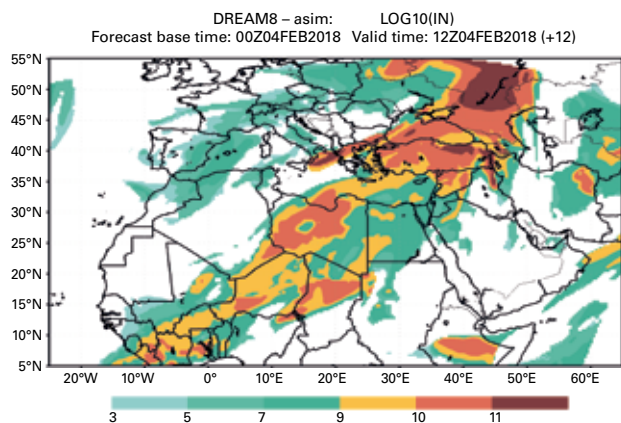


Figure 12. Example of predicted and observed cold cloud cover. Left: predicted load of Log10 (IN); right: observed via MSG-SEVIRI Ice Water Path. (Source: S. Nickovic)

towards using predicted IN concentration as an input in the cold cloud physics model (Figure 12).

PRIORITY AREA: Advance method

PREDICTABILITY IN SUB-SEASONAL-TO-SEASONAL FORECASTS

Starting from the assumption that aerosol effects can be more important at longer timescales, Benedetti and Vitart (2018) investigated whether aerosol variability could afford some predictability in sub-seasonal-to-seasonal forecasts. Twelve years of reforecasts with 50 ensemble members were analysed on a monthly scale. The results indicated that interactive aerosols are capable of improving sub-seasonal predictions at monthly scales for the spring/summer season. As an additional benefit, the authors demonstrated the possibility of making skilful dust forecasts at monthly scales, as illustrated in Figure 13.

SEASONAL ASIAN DUST PREDICTION IN EAST ASIA

In the SDS-WAS Asian Node, the Korea Meteorological Administration (KMA) has been carrying out seasonal forecasting of Asian dust using statistical techniques such as genetic algorithm and deep learning. To compensate for the shortcomings of these statistical methods, KMA started numerical model-based seasonal forecasting of Asian dust using the Global Seasonal Forecasting System

(GloSea5), a dynamics-based seasonal prediction model used operationally by KMA (Ryoo et al., 2020). To improve the model’s performance in Asia, the Asian node team at KMA replaced the dust generation algorithm GloSea5 over the East Asia region with the dust generation algorithm of the Asian Dust and Aerosol Model version 3 (ADAM3). The hindcast climatology for the spring-mean dust amount was constructed for the 20 years from 1991 to 2010 using GloSea5-ADAM (Figure 14). Figures 14b) to 14d) show the predicted dust anomalies for spring 2017, spring 2018 and spring 2019, respectively. This seasonal Asian dust prediction study by the SDS-WAS Research and Application Team is a positive step towards long-term SDS prediction.

IMPACT OF AEROSOLS ON WEATHER FORECASTING

The influence of aerosols on the forecast of meteorological elements is an essential issue for chemical weather forecasting. Simulation studies by a two-way coupled mesoscale weather-chemical model, GRPAES_CUACE, by the China Meteorological Administration (CMA), which includes sea salt, sand/dust, black carbon, organic carbon, sulphates, nitrates and ammonium product (Wang et al., 2018), show that aerosol particles, including dust, can induce or strengthen the local thermal inversion, affording humidification in the layer of aerosol primarily due to the aerosol-radiation interaction during a heavy aerosol pollution episode (HPE) of a duration of at least three days in the North China Plain. Understanding this two-way feedback effect between heavy aerosol pollution and meteorological conditions in the planetary boundary layer (Zhong et al., 2017; Wang et al., 2015; Zhang et al., 2019) is crucial for improving simulation and forecasting of the underestimated explosive growth of aerosols (Figure 15), and even weather forecasting during HPEs.

PRIORITY AREA: New observation

NEW INSTRUMENTAL DEVELOPMENTS TO MEASURE ATMOSPHERIC MINERAL DUST

The new ZEN-R52 multichannel radiometer is an improvement on the ZEN-R41 version (Almansa et al., 2017). The new radiometer has been specifically designed to monitor dust aerosols and atmospheric water vapour in remote desert regions with a high degree of autonomy and robustness (Almansa et al., 2020). The zenith sky radiance (ZSR) measurements of the ZEN-R41 prototype and the new ZEN-R52 radiometer have been compared with a collocated Aerosol Robotic Network (AERONET) Cimel CE318 (CE318-AERONET).

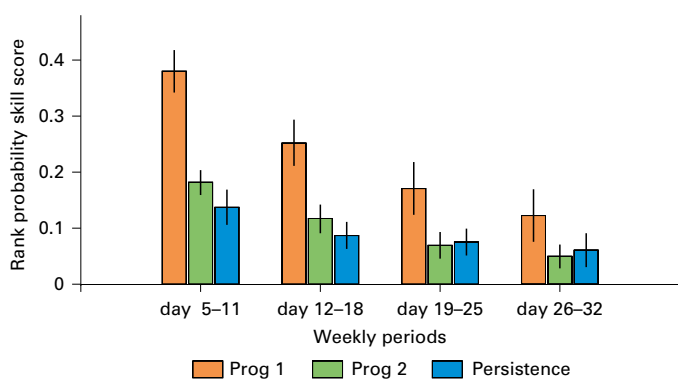


Figure 13. Skill of the dust forecast over one month measured by the ranked probability skill score (RPSS) for the experiments PROG1 (orange), in which the aerosols were initialized using the CAMS Interim Reanalysis, and PROG2 (green), in which the aerosols were initialized with an aerosol climatology, with respect to a persistence forecast (blue) of dust optical depth for the tropics. (Source: Benedetti and Vitart, 2018)

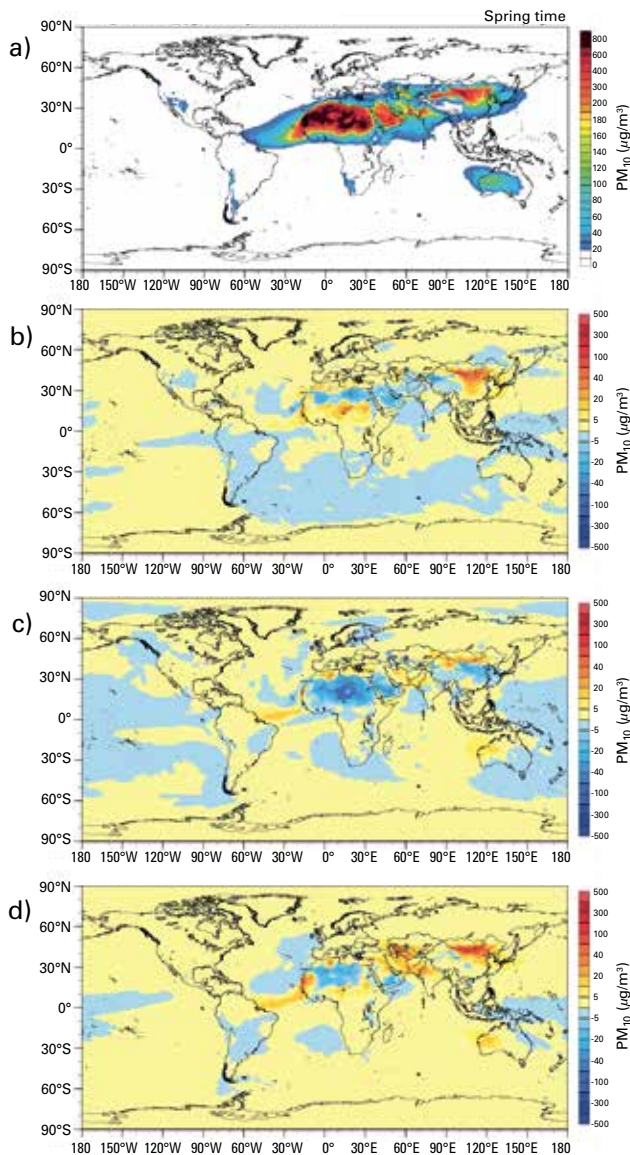


Figure 14. Seasonal forecasting of Asian dust using GloSea5-ADAM. a) is the average dust concentration from 1999 to 2010 (hindcast). b), c) and d) show the difference between the forecast level and the hindcast value for 2017, 2018 and 2019, respectively. (Source: Ryoo et al., 2020)

The results from the 10-month period from August 2017 to June 2018 show an improved performance of the ZEN-R52 compared with previous versions.

Spectral direct UV-visible normal solar irradiance (DNI) measured with an EKO MS-711 spectroradiometer at Izaña Atmospheric Observatory (IZO, Spain) has been used to determine spectral AOD in the entire spectral range (300 to 1 100 nm) (García-Cabrera et al., 2019). The EKO-711 DNI spectroradiometer has been designed for solar radiation monitoring, so its field of view (FOV=5) is twice that which is recommended for sun photometers by WMO for AOD determination. The AOD comparison from EKO-711 DNI spectroradiometers with AERONET at Izaña Atmospheric Observatory between April and September 2019 showed very good agreement (Figure 16).

OBSERVATION SUPPORT OF AEROSOL RADIATIVE PROPERTIES FROM CARSNET, CMA TO SDS-WAS

Sun photometers (CE-318, Cimel Electronique, Paris, France) were first installed at 20 China Aerosol Remote Sensing Network (CARSNET) sites in 2002 and have now been

installed at a total of 50 CARSNET sites (Figure 17). These sites include five sites in desert regions affected by mostly dust aerosols and two sites in regions affected by both dust and anthropogenic activities on the Loess Plateau. The AODs and extinction Ångström exponents (EAEs) at these sites varied from 0.21 to 0.60 and 0.25 to 1.03, respectively. The fine-mode fractions (FMFs) were 0.35 to 0.78, suggesting that there were higher relative abundances of mineral dust at these sites than at other sites in eastern and southern China. The annual single-scattering albedos (SSAs) at these sites were about 0.86 to 0.92, which demonstrates the scattering and absorption capacities of mineral aerosols in different regions. Indeed, in the spring, dust aerosols with light-absorbing properties occur more frequently in north-eastern China than in the southern areas, leading to the absorption aerosol optical depth (AAOD) values being about 0.02 to 0.05. A large direct aerosol radiative effect at the bottom of the atmosphere (DARE-BOA) (~ -37.14 to -91.20 W m⁻²) occurred around this region, and this fact implied a substantial surface cooling effect caused by mineral dust. A classification method based on SSAs, FMFs and EAEs showed that coarse-mode particles (mainly dust) (Group VII, EAE ≤ 0.60 , SSA ≤ 0.95) were dominant at the arid and semi-arid sites, with proportions of about 35% to 20% at most sites, with FMFs being 0.40 to 0.50.

Collaboration with United Nations Coalition to Combat Sand and Dust Storms

A United Nations Coalition to Combat Sand and Dust Storms was formally launched on 6 September 2019 at the 14th Conference of Parties (COP14) to the United Nations Convention to Combat Desertification (UNCCD) in New Delhi, India. At launch, the Coalition comprised 15 member organizations, including WMO, UNCCD and the United Nations Environment Programme (UNEP). The Coalition has a mandate to promote and coordinate a collaborative United Nations system response to SDS issues at local, regional and global levels, to facilitate the exchange of knowledge, data and best practices among Coalition members, to encourage collaboration on initiatives and action among Coalition members regarding SDSs, to facilitate dialogue and collaboration among affected countries and within the United Nations system with respect to SDS issues, to facilitate capacity-building in Member States, and to raise Member States' awareness of SDSs and enhance their preparedness for and response to SDSs. The Coalition has adopted a disaster risk management life cycle approach to its work and has created five working groups: Prevention, Mitigation, Preparedness, Response and Recovery. The WMO SDS-WAS Steering Committee (SC) will be leading the Preparedness working group.

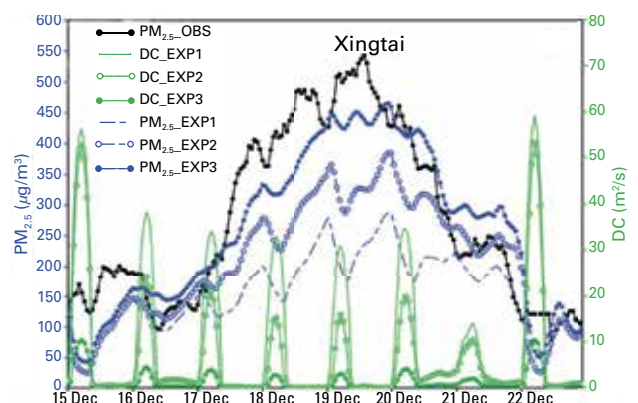


Figure 15. Hourly changes of PM_{2.5} and the diffusion coefficient (DC) of experiments EXP1, EXP2, and EXP3 from 15 to 22 December 2016 in Xingtai. (Source: Wang et al., 2018)

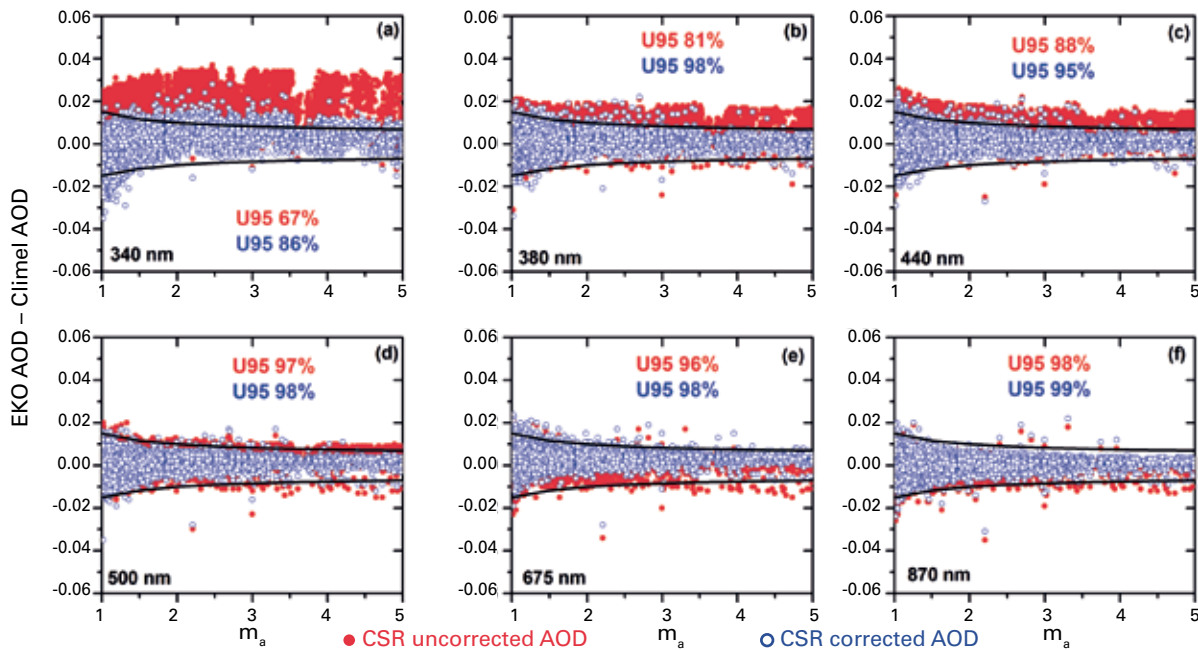


Figure 16. AOD differences (EKO AOD – Cimel AOD) versus optical air mass (m_a). The black lines represent the U95 uncertainty limits. (Source: García-Cabrera et al., 2019)

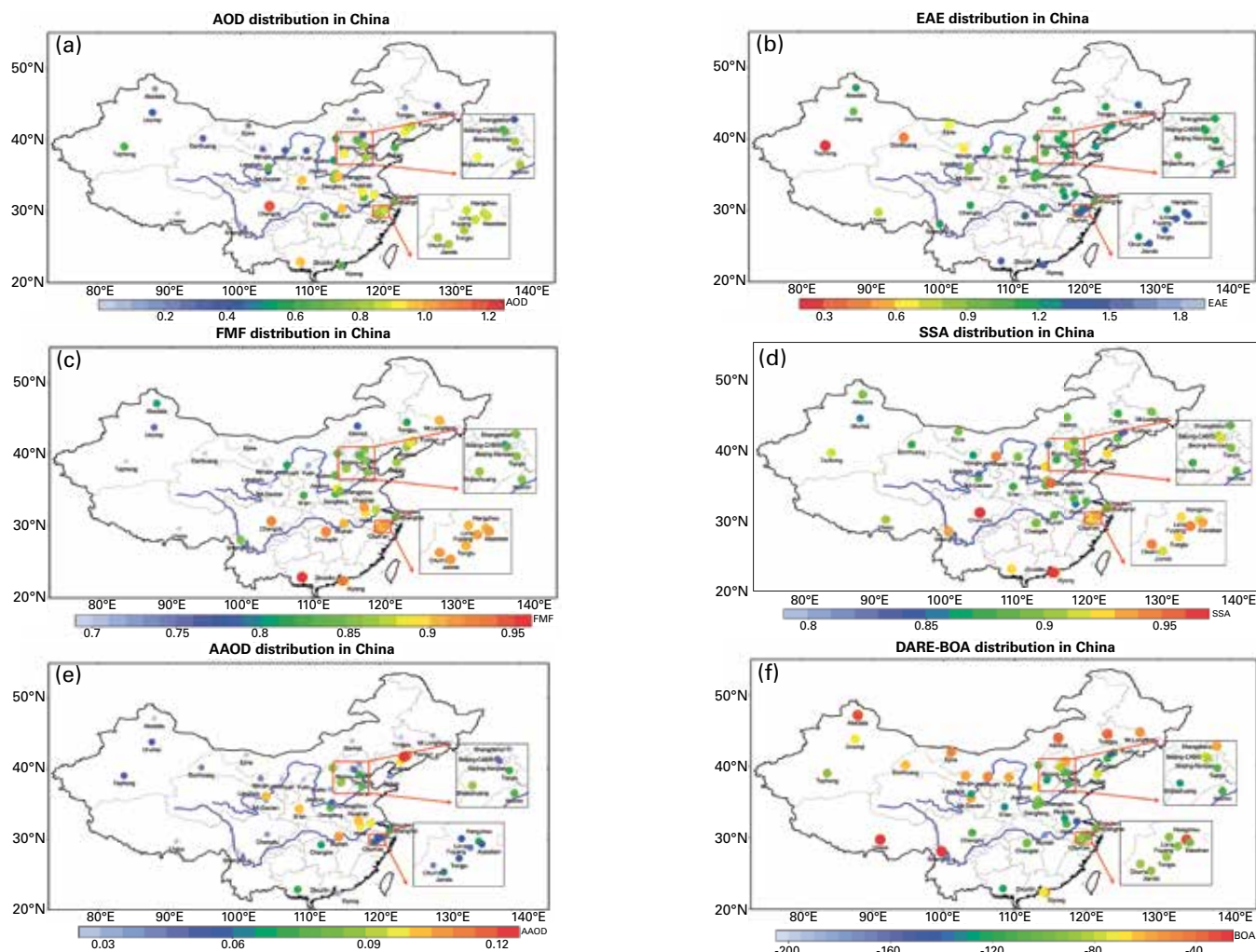


Figure 17. Annual spatial distributions of (a) aerosol optical depth (AOD) at 440 nm, (b) extinction Ångström exponent (EAE) 440–870 nm, (c) fine-mode fraction (FMF), (d) single-scattering albedo (SSA) at 440 nm, (e) absorption aerosol optical depth (AAOD) at 440 nm, and (f) direct aerosol radiative effect at the bottom of the atmosphere (DARE-BOA) at 50 China Aerosol Remote Sensing Network (CARSNET) sites. (Source: Che et al., 2019)

In the fifth session of the SDS-WAS SC (Hangzhou, China, 13–14 November 2019), SDS-WAS SC, the representatives of UNCCD, UNEP and the Economic and Social Commission for Asia and the Pacific/Asian and Pacific Centre for the Development of Disaster Information Management

(ESCAP/APDIM) introduced the Coalition's ongoing and future SDS projects and activities. The representatives expressed their willingness to strengthen cooperation with SDS-WAS. SDS-WAS SC suggested increasing the role and the contribution of SDS-WAS in the United Nations Coalition

to Combat Sand and Dust Storms and increasing collaboration with other partners in the areas of SDS impact-based warning, assessment and source management.

Within the United Nations Coalition to Combat Sand and Dust Storms, ESCAP/APDIM is trying to facilitate a regional plan of action for information sharing and capacity development related to combating SDSs in Asia and the Pacific. SDS-WAS SC suggests sharing data with ESCAP/APDIM in the 10–15 year long-term reanalysis of SDSs in the Asian area. This information will help ESCAP/APDIM plan for a longer-term overview of the hazardous impacts of SDSs in specific locations in the

Asia Pacific region. The Japan Meteorological Agency (JMA), representing SDS-WAS, will share SDS reanalysis data at 120-60 km resolution with ESCAP/APDIM by 2021.

SDS-WAS SC also discussed with the representative of UNCCD collaborating and sharing the data obtained from a 1-km global map of SDS sources coordinated by UNCCD. This is another concrete action which would strengthen cooperation within the United Nations Coalition to Combat Sand and Dust Storms in order to better forecast SDSs in areas where sources change greatly and in order to better forecast small-scale SDS events, such as haboobs.

References

- Almansa, A.F., et al., 2017: A new zenith-looking narrow-band radiometer-based system (ZEN) for dust aerosol optical depth monitoring. *Atmos. Meas. Tech.*, 10(2): 565-579.
- Almansa, A.F. et al., 2020. Column Integrated Water Vapor and Aerosol Load Characterization with the New ZEN-R52 Radiometer, *Remote Sens.*, 12, 1424.
- Benedetti, A., Vitart, F., 2018. Can the Direct Effect of Aerosols Improve Subseasonal Predictability? *Monthly Weather Review*, 146.
- Che, H. et al., 2019. Spatial distribution of aerosol microphysical and optical properties and direct radiative effect from the China Aerosol Remote Sensing Network. *ACP* 19(18): 11843-11864.
- Cziczo, D.J. et al., 2013. Clarifying the Dominant Sources and Mechanisms of Cirrus Cloud Formation. *Science*, 340(6138): 1320-1324.
- Demott, P.J. et al., 2015. Integrating laboratory and field data to quantify the immersion freezing ice nucleation activity of mineral dust particles. *ACP*, 15(1): 393-409.
- Flemming, J. et al., 2017. The CAMS interim Reanalysis of Carbon Monoxide, Ozone and Aerosol for 2003–2015. *ACP*, 17(3): 1945-1983.
- García-Cabrera, R.D. et al., 2019. Characterization of an EKO MS-711 spectroradiometer: aerosol retrieval from spectral direct irradiance measurements and corrections of the circumsolar radiation. *Atmos. Meas. Tech. Discuss.*, 2019: 1-26.
- Gelaro, R. et al., 2017. The Modern-Era Retrospective Analysis for Research and Applications, Version 2 (MERRA-2). *J. of Climate*, 30(14)
- Ginoux, P. et al., 2012. Global-scale attribution of anthropogenic and natural dust sources and their emission rates based on MODIS Deep Blue aerosol products. *Rev. of Geoph.*, 50(3).
- Jugder, D. et al., 2018. Developing a soil erodibility map across Mongolia. *Natural Hazards*.
- Klose, M. et al., 2014. Further development of a parameterization for convective turbulent dust emission and evaluation based on field observations. *JGR Atmospheres*, 119(17): 10441-10457.
- Liu, J. et al., 2002. The land use and land cover change database and its relative studies in China. *J. of Geogr. Sci.* 3: 275-282.
- Nickovic, S. et al., 2016. Cloud ice caused by atmospheric mineral dust - Part 1: Parameterization of ice nuclei concentration in the NMME-DREAM model. *ACP*, 16: 11367-11378.
- Nickovic, S. et al., 2015. Modelling ice nucleation due to dust, *EGU2015*.
- Ren, Y. et al., 2019. Effects of turbulence structure and urbanization on the heavy haze pollution process. *ACP*, 18(23): 17717-17733.
- Ryoo, S. et al., 2020. Seasonal Asian Dust Forecasting Using GloSea5-ADAM. *Atmosphere*, 11, 526
- Steinke, I. et al., 2016. A new temperature- and humidity-dependent surface site density approach for deposition ice nucleation. *ACP*, 15(7): 3703-3717.
- Tackett, J.L. et al., 2018. CALIPSO lidar level 3 aerosol profile product: version 3 algorithm design. *AMS*, 11(7): 4129-4152.
- Wang, H. et al., 2018. Contributions to the explosive growth of PM_{2.5} mass due to aerosol-radiation feedback and decrease in turbulent diffusion during a red alert heavy haze in Beijing-Tianjin-Hebei, China. *ACP*, 18(23): 17717-17733.
- Wang, H. et al., 2015. Mesoscale modelling study of the interactions between aerosols and PBL meteorology during a haze episode in China Jing-Jin-Ji and its near surrounding region: Aerosols\ radiative feedback effects. *ACP*, 15(6): 3277-3287.
- Zhang, X. et al., 2019. Airborne Dust Bulletin No. 3, WMOI, https://library.wmo.int/doc_num.php?explnum_id=6268
- Zhang, Z. et al., 2014. A 2010 update of National Land Use/Cover Database of China at 1:100000 scale using medium spatial resolution satellite images. *RSE*, 149: 142-154.
- Zhong, J. et al., 2017. Relative Contributions of Boundary-Layer Meteorological Factors to the Explosive Growth of PM_{2.5} during the Red-Alert Heavy Pollution Episodes in Beijing in December 2016, *J. Meteor. Res.*, 31(5): 809-819.
- Zhou, C. et al., 2019. Detection of new dust sources in central/East Asia and their impact on simulations of a severe sand and dust storm. *JGR: Atmospheres*, 124.

WMO SDS-WAS websites and contacts

WMO SDS-WAS:

<http://www.wmo.int/sdswas>
email: abaklanov@wmo.int

Regional Centre for Northern Africa, Middle East and Europe (NAMEE):

<http://sds-was.aemet.es> and <http://dust.aemet.es>
email: sdswas@aemet.es

Regional Centre for Asia:

<http://www.asdf-bj.net/>
email: xiaoye@cma.gov.cn

Regional Centre for Americas:

<http://sds-was.cimh.edu.bb/>
email: asealy@cimh.edu.bb

Editorial board

Xiaoye Zhang (Chinese Academy of Meteorological Sciences, CMA), Slobodan Nickovic (Republic Hydrometeorological Service of Serbia), Ernest Werner (State Meteorological Agency of Spain), Sang Boom Ryoo (National Institute of Meteorological Sciences, KMA), Andrea Sealy (Caribbean Institute for Meteorology and Hydrology), Alexander Baklanov (WMO)

All authors

Xiaoye Zhang, Slobodan Nickovic, Ernest Werner, Angela Benedetti, Sang Boom Ryoo, Gui Ke, Chunhong Zhou, Tianhang Zhang, Emilio Cuevas, Huizheng Che, Hong Wang, Sara Basart, Robert Green, Paul Ginoux, Lichang An, Lei Li, Nick Middleton, Takashi Maki, Andrea Sealy, Alexander Baklanov